DOI: 10.2352/ISSN.2470-1173.2016.13.IQSP-203

Correlation of Photo-Response Blooming Metrics with Image Quality in CMOS Image Sensors for Mobile Photography

Pulla Reddy Ailuri, Orit Skorka, Ning Li, Radu Ispasoiu, and Vladi Korobov
Image Sensor Group, ON Semiconductor, San Jose, CA, USA

Abstract

Pixel blooming in CMOS image sensors is often characterized by metrics that are extracted from the photo-response curve. This work explores whether these pixel blooming metrics are in any significant correlation with end-user image quality in mobile photography, and provides quantitative answers to that question by studying changes in size and color of saturated image regions.

Introduction

The continuing development in the technology of sub-2 µm pixel CMOS image sensors (CIS) for mobile imaging requires accurate characterization techniques and metrics that capture the correlation between pixel performance and end-user image quality [1], [2]. One of the important sensor performance properties is pixel blooming. Pixel blooming can be fundamentally defined as the mechanism governing the spreading of charge from one pixel to its neighbors in an amount that is beyond the point-spread-function of the pixel, in exposure conditions where photo-generated charge exceeds the pixel full-well capacity. While there are several techniques to characterize image sensor pixel blooming, metrics that are based on photo-response curves are commonly used with CIS for mobile imaging applications. However, correlation between these metrics and actual image quality performance has so far not been addressed in the literature.

This work investigates whether there is a correlation between photo-response blooming metrics and two important end-user image quality parameters that are affected by saturation artifacts: size of saturated region in the image, and color difference. Results are shown for experimental work that was done with sensors for mobile photography.

Response-Slope Blooming Metrics

Blooming metrics are calculated from signal responses. While illuminance level is kept constant, integration time is swept and the signal of a central region of interest is measured for all the color planes. The sweep is extended until all the color planes are saturated. CIS which exhibits pixel blooming will show the change in signal slope for unsaturated pixels after one color plane saturates.

Figure 1 shows the response and response-slope of the four color planes versus integration time of a 1.1 µm pixel sensor under illumination from a green light-emitting diode. After green pixels reach saturation, one may observe a change in the response-slope of red and blue pixels.

Several blooming metrics have been proposed to quantify the magnitude of this change in slope. When referring to the example shown in Figure 1, the metric used by Chao et.al [3] is defined as:

$$M_1 = (S_{B\_max}\text{-}S_{B\_NB})/S_{G\_NB,} \quad (1)$$

where S_{B_max} is the maximal slope and S_{B_NB} is non-blooming slope of the blue color plane, and S_{G_NB} is the non-blooming slope of the green plane. The metric used by Sengoku et. al [4] is defined as

$$M_2 = (S_{B\_max}\text{-}S_{B\_NB})/S_{B\_NB.} \quad (2)$$

The metric that is used in this work is defined as:

$$M_3 = S_{B\_max}/S_{B\_NB.} \quad (3)$$

Although the metrics are demonstrated here on the blue plane under green light illumination, the same equations are valid for all color planes, and are not limited to green light.

With the metrics described in (1) and (2), metric value is 0 for blooming-free pixels, whereas with the metric that is described in (3), metric value is 1 for blooming-free pixels (or perfect anti-blooming).

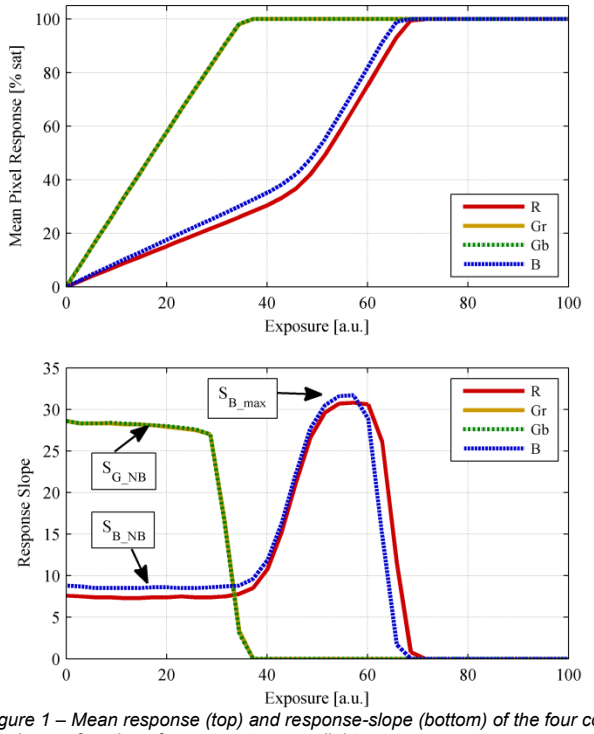

Figure 1 – Mean response (top) and response-slope (bottom) of the four color pixels as a function of exposure to green light.

©2016 Society for Imaging Science and Technology
DOI: 10.2352/ISSN.2470-1173.2016.13.IQSP-203

Pixel Settings Trade-Offs

Figure 2 presents the basic 4T pixel circuit and its timing diagram. Pixel operation starts by resetting the photo-diode (PD) by simultaneously turning on the reset (RST) and transfer gate (TX) transistors. RST and TX transistors are then turned off to start charge integration in the PD. Once integration time is completed, the RST transistor is turned on to reset the floating diffusion (FD), and the reset signal level is sampled by turning on the row select (RS) transistor. After reset level sampling, the signal level is sampled by turning on the TX and RS transistors. This mode of operation is called correlated double sampling (CDS), and its purpose is to eliminate reset noise.

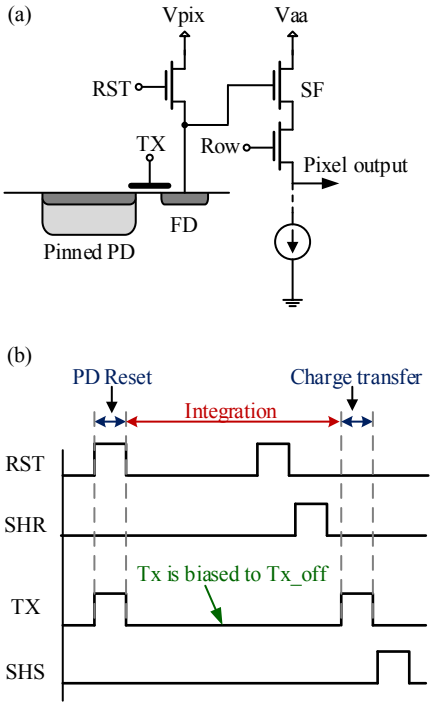

Figure 2 – 4T pixel circuit (a) and timing diagram (b). During integration time, the transfer gate is biased to Tx_off voltage.

Pixel blooming can be controlled by varying the TX voltage during charge integration, Tx_off. As Tx_off is biased to more positive voltages, the potential barrier between PD and FD (under Tx) is reduced. This facilitates leakage of charge from PD to FD during integration time. Therefore, in this condition, when a pixel PD is close to reaching its full well capacity, charge leakage to the pixel's own FD is greater than charge leakage into PDs of neighboring pixels and consequently the blooming metrics (1) – (3) are reduced towards their lowest limits.

Figure 3 shows the response of the red plane for different Tx_off voltage levels and that of the green plane when Tx_off is biased to the most negative voltage. The same figure also shows a blooming metric plot that was calculated according to (3). One may conclude that change in the response slope of the red color plane is diminished as Tx_off becomes more positive and its M_3 blooming metric is getting closer to 1.

Use of more positive Tx_off voltage levels reduces pixel blooming but it comes at the cost of reduction in the pixel linear full well, increase in dark current and increase in number of bright pixels. With the sensor that was characterized in **Figure 3**, for example, the M_3 blooming metric is 1 when Tx_off is biased to a voltage of $-V_{max}$ + 60% of ΔV. However, under the same operating conditions the LFW drops by 20%, the dark current becomes 20 times higher, and bright pixel count increases by a factor of 100.

Output values of the three blooming metrics that are described in the above sections are not comprehensive. They vary with illuminant spectra, illuminance intensity, optical cross-talk and full well capacity.

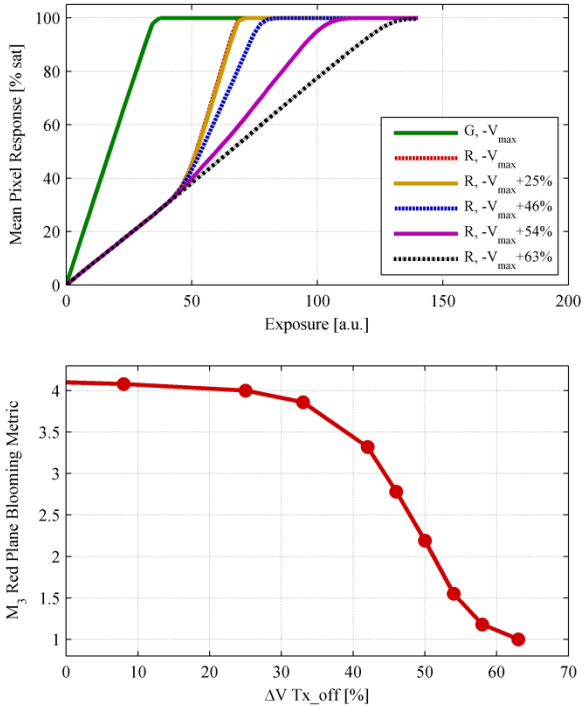

Figure 3 – Change in mean response of green and red with exposure to green light for different Tx_off voltage levels (top). Red pixel blooming response-slope ratio for different Tx_off voltage levels (bottom). Note that when the voltage is increased by 63% of entire voltage range, there is no change in slope after green pixels reach saturation.

Blooming-Related Image Artifacts

One of the expected image artifacts that can result from pixel blooming and applies to both monochrome and color sensors is the increase in the size of a saturated region in the image due to photodiode wells that are filled by leak of charge from adjacent photodiodes rather than by optical generation. In color sensors, saturation artifacts can result in increase of color difference. White-balance and color correction coefficients that are used with any color imaging pipeline are optimized to achieve high color accuracy, under certain constraints, according to the relative response of the different color pixels in non-saturating conditions. The imaging pipeline expects the relative response to remain constant, and any divergence due to charge leakage can lead to degradation in color reproduction.

The goal of this work is, therefore, to understand and quantify the answer to the question whether imperfect score on photo-response blooming metrics (i.e. larger than minimum values on the M_1-M_3 metrics) is correlated with end-user noticeable image artifacts. The following sections are defining characterization methods for 1) saturated region size, and 2) color difference to provide quantitative answers to the question above.

DOI: 10.2352/ISSN.2470-1173.2016.13.IQSP-203

Size of Saturated Region

To study the effect of blooming on change in the size of saturated regions in captured images, we designed a setup that allows maintaining a constant well-defined size of an illuminated area on the image plane while varying light irradiance. In order to determine if a pixel reaches saturation due to blooming rather than optical generation, the expected optical response is calculated by multiplying the image that was captured with low light intensity by the power ratio. This is compared to the actual image that was captured with high intensity. The difference is considered a quantitative measure of pixel blooming.

A laser beam was used in the experiment to illuminate a small region on the image plane. The lab setup is shown in

Figure *4*; it includes a red HeNe laser (632.8 nm), and a neutral density (ND) filter for irradiance control. A beam splitter, which is made of a coated piece of thin glass, is used to direct a portion of the beam to a silicon photodiode in order to monitor the relative power density of the light that arrives at the image plane in real time. An iris diaphragm and a lens are used to produce an illuminated region on the image plane with diameter that does not exceed 10 μm.

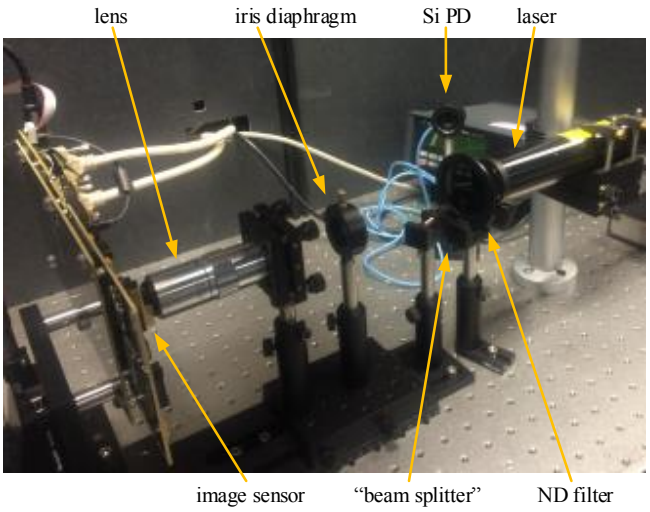

Figure 4 – Laser setup for characterization of increase in size of saturated regions as an outcome of pixel blooming.

Integration time was adjusted to match typical values that are used in outdoor imaging conditions when saturation artifacts are likely to occur, such as reflections of sun light from cars. It was kept constant during the experiment, so that the same integration time was used with all image captures.

Two image sets of the saturated region were captured. Each set includes 16 images that differ by the Tx_off bias voltage that was used during capture, and covers a voltage range that starts with the most positive and ends with the most negative levels in order to sweep for conditions from perfect anti-blooming to maximum pixel blooming. The laser beam was attenuated in both sets using an ND filter. With the first image set, a power density of $P_1 = P_0$ was read on the reference silicon photodiode. An ND filter with lower attenuation was used with the second image set, and the reference PD showed power that was 6.33 times higher, i.e., $P_2 = 6.33 \cdot P_0$. The two image sets are shown in **Figure 5**.

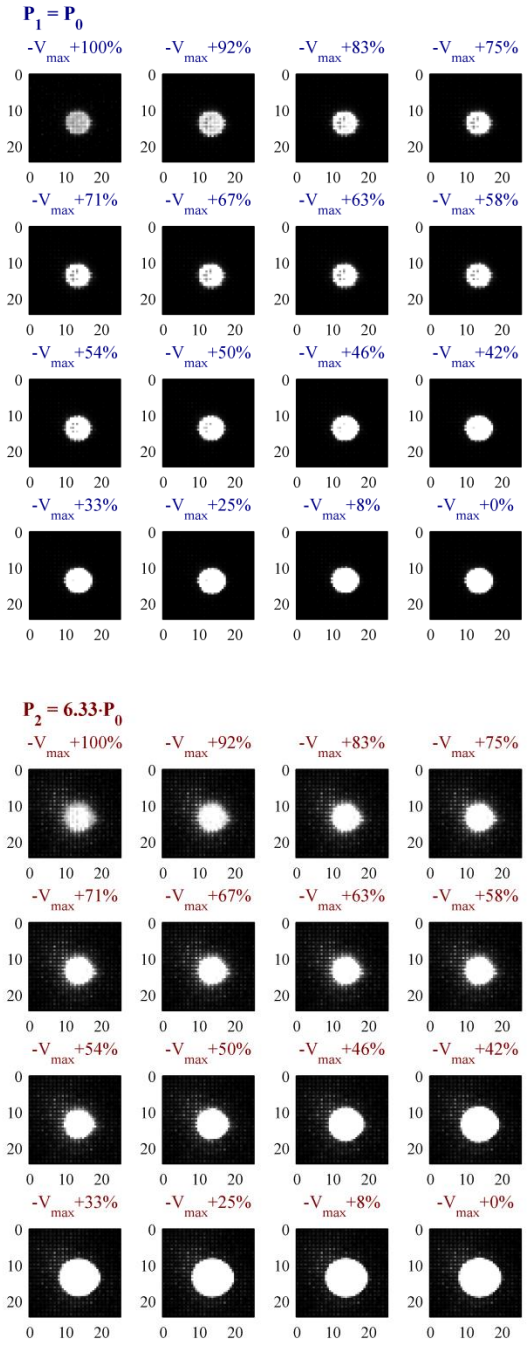

Figure 5 – Two sets of laser spot images were captured with 16 Tx_off bias levels that ranged from the most positive (-V_{max}+100%) to the most negative (-V_{max}+0%) ones. Power density of incident light that was used with the second set was 6.33 times higher than the initial power density, i.e., $P_1 = P_0$ and $P_2 = 6.33P_0$.

To determine the effect of blooming, a third "synthetic" image set was prepared by multiplying digital values of all images that were captured with light intensity P_1 by the power ratio 6.33 – in order to simulate the expected spot size due to pure optical saturation. Digital pixel values were then truncated to the maximal digital value of the sensor, as dictated by bit resolution of the analog-to-digital converter and the pedestal level. **Figure 6** shows

DOI: 10.2352/ISSN.2470-1173.2016.13.IQSP-203

the difference images that are obtained by subtracting the calculated image from the captured one for each Tx_off bias level. All the pixels in these images whose digital value is greater than 1 are affected by blooming, as some of the charge that is accumulated in their well was not optically-generated at the same pixel area.

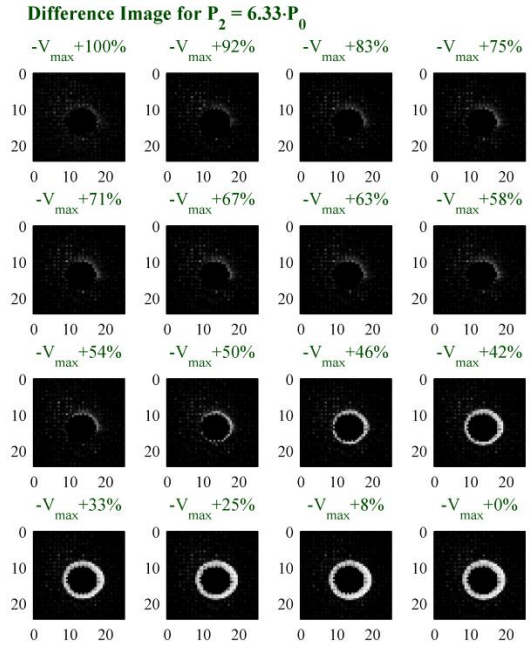

Figure 6 – The difference image represents the difference between the calculated image, as obtained by multiplying the low power image by the power ratio, and the captured high power image.

Figure 7 shows the total number of pixels, S_{sat}, that reach saturation in each one of the images in the three image sets. It also shows the effective radius of each image, which was calculated as follows:

$$r_{eff} = \sqrt{S_{sat}/\pi} \quad (4)$$

Results show that blooming occurs when Tx_off is biased to voltages < -V_{max} + 54% of ΔV. For all voltage levels that are more negative than this value, there is a clear difference between S_{sat} of the captured image and S_{sat} of the calculated one. With the most positive Tx_off bias levels, there is spill of charge to the floating diffusion capacitance. Therefore, S_{sat} is lower than expected. The quantitative answer to the question of image correlation with pixel blooming is that, even when the most negative voltage is applied to Tx_off, the difference in r_{eff} does not exceed 3 pixels. In a mobile imaging mega pixel sensor, such a difference has a barely noticeable effect on the final image.

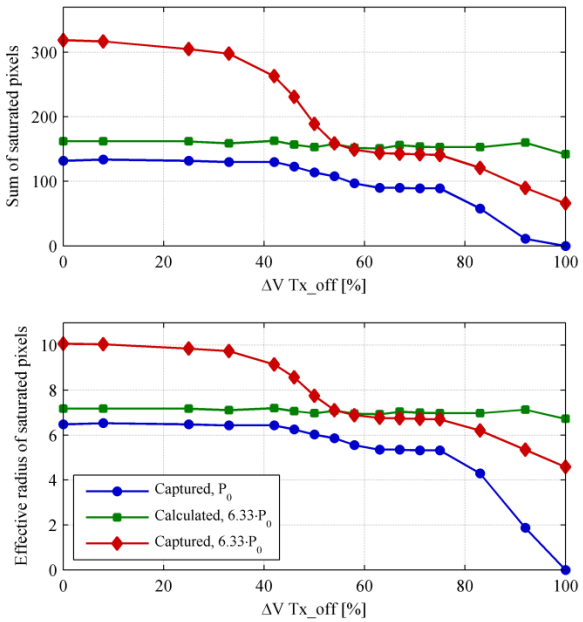

Figure 7 – Sum (top) and effective radius (bottom) of the saturated region on the image plane versus relative voltage level on the Tx_off gate for the three image sets.

Color Difference

To investigate correlation between pixel photo-response blooming metrics and degradation in color accuracy under saturation, a set of Macbeth color checker chart images was captured with two sensors under conditions of variable exposures. The choice of sensors for this study was as follows: Sensor A shows a notable change in slope when one channel reaches saturation and, therefore, metrics M_1-M_3 have relatively high values, while those metrics are at their minimum values for Sensor B. The two image sets are shown in **Figure 8.**

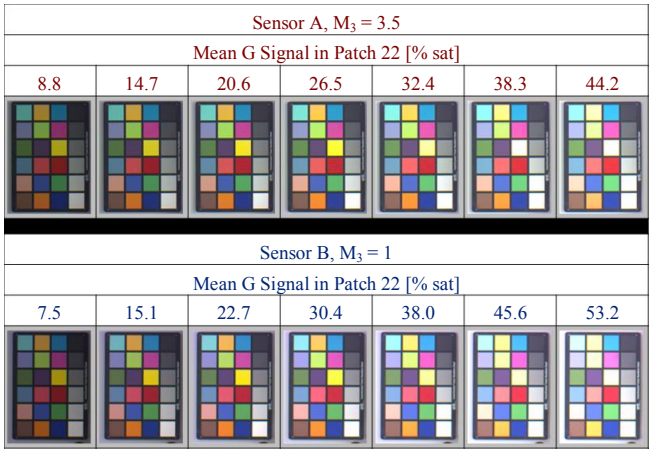

Figure 8 – Macbeth-chart images were captured with the two sensors under a GTI-3000K illuminant. Integration times were varied to produce an image set from under-exposed to over-exposed images. While Sensor A shows change in response –slope after one color channel reaches saturation, Sensor B does not.

All image captures were done when both analog gain and global digital gain were set to 1. The chart was placed on a wall of

DOI: 10.2352/ISSN.2470-1173.2016.13.IQSP-203

a light box that was illuminated by a GTI-3000K under constant illuminance. Images were saved in raw data format, and color processing was done off-line.

To determine white-balance gain (WBG) and color-correction matrix (CCM) coefficients, one image was captured with each sensor after integration time was adjusted so that mean green pixel response in the white patch of the Macbeth chart (patch 19) was at about 90% of saturation. WBG coefficients were chosen to achieve equal signal level for all color planes in the gray-scale patches (patches 19-24). CCM coefficients were optimized according to tabulated RGB values of each patch. These coefficients were used to process all raw images that were captured with the same sensor. Patch order in a Macbeth chart is shown in **Figure 9**.

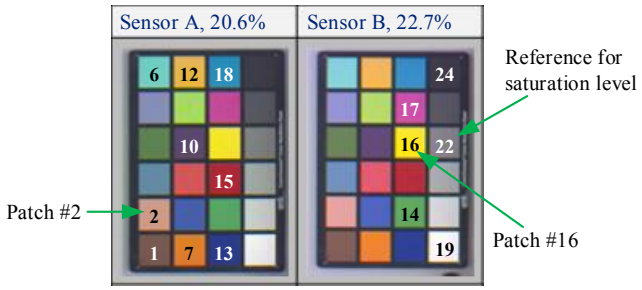

Figure 9 – Macbeth chart patch numbers. The two charts were captured with sensors A and B, where saturation level in patch 22 is 20.6% and 22.7%, respectively. Color difference values are later shown for patches 2 and 16.

Raw images of both sensors were processed with a basic pipeline that included de-mosaicing, white-balancing, color correction, and standard gamma correction. For a fair comparison and in order to exclude the effect of sensitivity differences between the two sensors, images are arranged according to saturation level of patch 22, which is a gray patch with 18% reflectance.

One may observe significant change in color due to saturation and blooming artifacts in patches 2 and 16 among the 18 color patches of the Macbeth color checker chart (patches 1-18). **Figure 10**(a) and (b) present the change in mean pixel response of the 4 color planes in patch 2 in images that were captured with Sensor A and B, respectively, vs signal saturation level in patch 22. **Figure 11**(a) and (b) presents the same properties for patch 16. **Figure 10**(c) and **Figure 11**(c) show color difference values, as calculated for these two patches according to the ΔE_{2000} standard *[5]*, **Figure 12** shows the root-mean-square (RMS) change in color difference for the 18 color patches of the chart.

Change in response slope of the blue plane after the red and green planes saturate in patch 16 images of Sensor A is obvious from **Figure 11**(a). Nonetheless, both sensors exhibit increase in color difference with exposure, where the error is slightly higher for Sensor B in patch 2 and for Sensor A in patch 16, and the overall performance is fairly similar, as may be concluded from **Figure 12**. The ΔE_{2000} standard accounts for differences in brightness (luma), hue, and colorfulness (chroma) between tabulated reference values and the sensor for each patch.

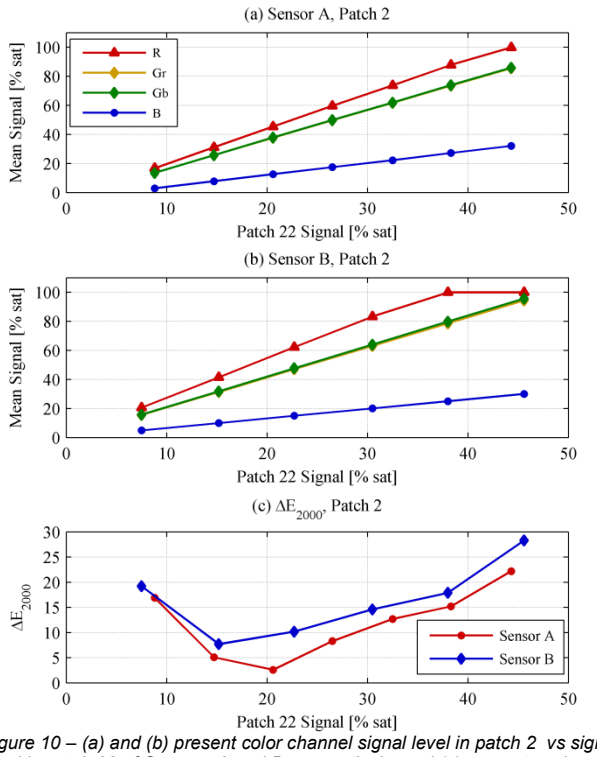

Figure 10 – (a) and (b) present color channel signal level in patch 2 vs signal level in patch 22 of Sensors A and B, respectively, and (c) presents color difference in patch 2 vs signal level in patch 22 of Sensors A and B.

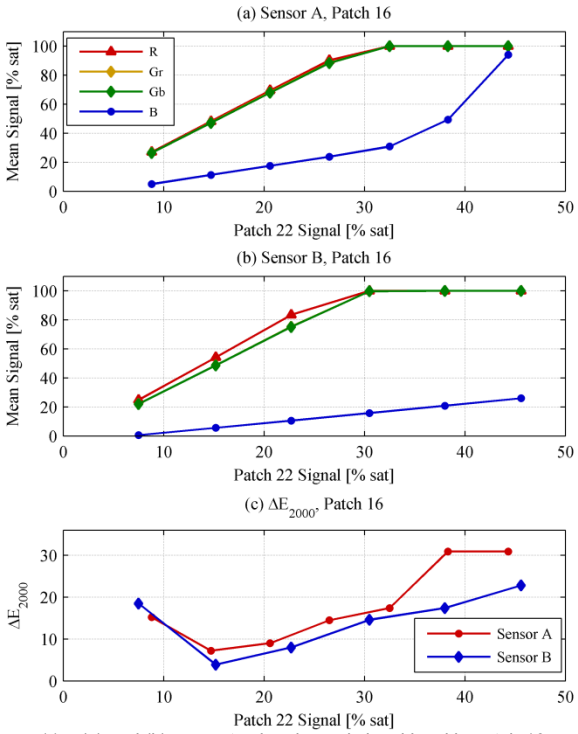

Figure 11 – (a) and (b) present color channel signal level in patch 16 vs signal level in patch 22 of Sensors A and B, respectively, and (c) presents color difference in patch 2 vs signal level in patch 22 of Sensors A and B.

DOI: 10.2352/ISSN.2470-1173.2016.13.IQSP-203

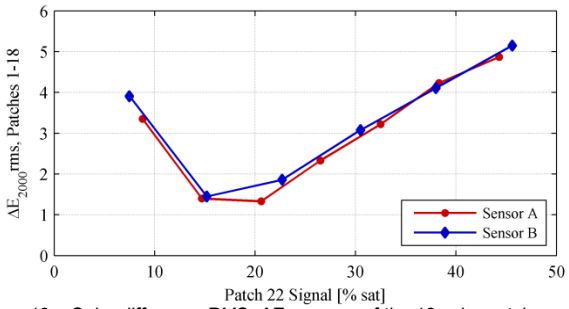

Figure 12 – Color difference RMS, ΔE_{2000}_rms, of the 18 color patches of the Macbeth chart vs signal level of patch 22. The two sensors achieve very similar overall performance.

With standard auto-exposure settings, integration time and gain are adjusted so that the mean green channel response after color processing is 18% of the maximal digital value of the sensor output before gamma correction, which corresponds to 22.5% signal saturation in patch 22 in the images above. Therefore, a well-designed auto-exposure control mechanism for mobile photography should eliminate increase in color difference due to saturation and blooming.

Conclusion

This work aimed to investigate the correlation between pixel photo-response blooming metrics and end-user image quality. For that purpose, experimental apparatus and image analysis methodology have been developed to examine the effect of pixel blooming on: 1) the size of saturated regions on the image plane, and 2) color difference. Results show that, even when the photo-response curve has high change in slope after one color plane saturates, the increase in radius of saturated regions is less than 5 pixels, which has negligible effect on image quality in mobile photography mega-pixel sensors. They also show that in terms of color performance, sensors with high values of the blooming metrics from equations (1) - (3) perform comparably to sensors with low values of the blooming metrics (perfect anti-blooming), because assumptions used by the color imaging pipeline regarding signal linearity and color plane sensitivity ratios become invalid after one color plane saturates regardless of the change in response of the non-saturated other planes.

Acknowledgment

The authors would like to thank Naoyuki Suzuki and Lidiya Polukhina for their contribution to the section that discusses the effect of saturation and blooming on color difference.

References

[1] V.-T. Peltoketo, "Mobile phone camera benchmarking in low light environment," in *Proceedings of SPIE-IS&T Electronic Imaging*, 2015.

[2] International Imaging Industry Association, "CPIQ Initiative Phase 1 White Paper: Fundamentals and review of considered test methods," Director of Standards, I3A, 2007.

[3] Calvin Chao, Kuo-Yu Chou, Charles Liu, Yi-Che Chen, Hon-Yih Tu,Hsiu-Yu Cheng, Fu-Lung Hsueh, and Shou-Gwo Wuu, "Blooming and Antiblooming in 1.1µm-Pixel CIS," in *International Image Sensor Workshop*, Utah, USA, 2013.

[4] M. Sengoku, H. Yoshimura, Y. Sugiura, S. Shimizu, R. Hasumi and M. Monoi, "Quantitative full 3D blooming analysis on 1.4um BSI CMOS image sensor," in *International Conference on Simulation of Semiconductor Processes and Devices (SISPAD)*, 2013.

[5] CIE, "Improvement to industrial colour-difference evaluation," CIE Publication No. 142-2001, Central Bureau of the CIE, Vienna, 2001.

Author Biography

Pulla R. Ailuri received his BS in Electronics and Communication Engineering from Osmania University, India, in 2005, and his MS in Electrical Engineering from New Mexico State University, USA, in 2008. His MS research work focused on dynamic current mirror active pixel image sensors. He joined Aptina in 2009 as a Product Engineer, and became a Pixel Characterization Engineer in 2013. He is now with the Image Sensor Group at ON Semiconductor.

Orit Skorka received her BSc from Ben-Gurion University of the Negev, Israel, in 2001, her MSc from the Technion IIT, Israel, in 2004, and her PhD from the University of Alberta, Canada, in 2011, all in Electrical and Computer Engineering. She joined Aptina in 2013 and is now with the Image Sensor Group at ON Semiconductor. She is working on pixel characterization and image quality of CMOS image sensors for mobile imaging and automotive applications.

Ning Li received his BS in Electrical Engineering from Xi'an Jiaotong University, China, in 2009, and his MS degree in Electrical and Computer Engineering from Tufts University, USA, in 2011. He is a Staff Characterization Engineer in the Image Sensor Group at ON Semiconductor. He is a part of the characterization and image quality team.

Radu Ispasoiu is senior manager of pixel R&D and image quality at ON-Semiconductor ISG (since 2014). He has held engineering management and lead R&D positions in Silicon Valley optoelectronics technology industry for more than 15 years. He holds a PhD in Physics (1996) with focus on semiconductor optoelectronic device study from the University of Oxford, UK.

Vladi Korobov is a senior director of advanced technology development at Image Sensor Group at ON-Semiconductor. He has led variety of senior management positions in semiconductor field. Vladi was involved in CMOS image sensors technology for more than 18 years. He holds a PhD in EE from Tel-Aviv University, Israel.